

Cement in-line calciner kiln modeling for heat optimization using a design of computer experiments

Alejandro Ortiz^{a,*}, Santiago Builes^b, Diego Acosta^b

^a*Cementos Argos S.A., Medellín, Colombia*

^b*Grupo de Investigación DDP, Universidad EAFIT, Medellín, Colombia*

November 10, 2020

Abstract

A model of a dry process cement kiln was implemented in Aspen Plus V9 and validated with a 2000 metric ton per day in-line calciner cement kiln data. A simplified model of the process was obtained using a 20-run Plackett-Burman design of experiments on Aspen Plus simulations with 19 input variables related to false air (in-leakage air), oxygen concentration, calciner temperature, cyclones efficiency and clinker's cooler bed height. Linear metamodells for the specific heat consumption (SHC) and other response variables were obtained. The metamodel indicated that (i) false air in cyclones 4 and 5, (ii) calciner's control temperature, (iii) oxygen concentration at the calciner exit and (iv) cooler's clinker bed height were the most significant input variables affecting SHC. The SHC obtained from simulation based on the optimized values from the metamodel resulted in a reduction of ca. 29 kcal/kg of clinker. A sensitivity analysis indicated that the two most impacting variables were the oxygen concentration at the calciner's exit and the cooler's clinker bed depth. The SHC metamodel is a powerful tool for capturing the complexity of the process simulations on a simple and easy to use model.

Keywords: Cement pre-calciner kiln, heat optimization, design of computer experiments, clinker model, Aspen Plus simulation, linear metamodel.

* Corresponding author.

E-mail addresses: aortiz@argos.com.co (Alejandro Ortiz), sbuiles@eafit.edu.co (Santiago Builes), dacostam@eafit.edu.co (Diego Acosta)

1 Introduction

Cement manufacturing is an energy intensive industry [1]. For instance, energy utilization in cement industry was reported to be 9.3 EJ/year during 2008, behind the iron and steel industries (25.9 EJ/year), petroleum refineries (12.1 EJ/year), but ahead of pulp and paper (7.8 EJ/year) and ammonia (6.5 EJ/year) industries [2].

Cement clinker is an intermediary synthetic product in the manufacture of Portland cement and is the main constituent of Ordinary Portland Cement (OPC). Clinker is produced by sintering a grinded blend of limestone, clay and iron ore (raw meal) in the cement kiln. The cement kiln is also the main consumer of thermal energy in this industry with a worldwide consumption of 3.9 GJ per metric ton of clinker, in a range from 2.9 GJ/t clinker to 6.6 GJ/t clinker [2]. Thus, heat and energy optimization are main concerns in clinker production as it can result in lower generation of combustion gases and higher clinker production.

A modern clinker manufacturing kiln can have several arrangements. A simple one consists of a suspension preheater (SP) tower, a calciner, a rotary kiln and a clinker cooler. A typical preheater tower has between 4 to 6 cyclone stages. The higher the number of stages, the higher the heat recovery from process gases coming from the kiln and the calciner; however, the chosen number of stages also depends on other process, and environmental and economic factors, such as the drying requirements of the raw material, the availability of local water resources (for cooling hot gases from preheater) or the price of the electricity.

Raw meal (kiln feed) is fed before the top stage in the preheater tower. A fraction of solids is captured in the cyclone and goes to the bottom to feed the second stage. This process is then repeated for each of the cyclone stages in the SP tower. The hot ascending gases preheat the solids as they fall through the battery of cyclones. Then, the collected solids in the next to last cyclone go to calciner where a partial limestone decarbonation occurs. After this, the solids go to the last cyclone and the fraction captured in this cyclone (hot meal) finally goes to the rotary kiln where decarbonation is finished and

clinkerization reactions take place. Hot clinker leaves the kiln to be cooled by ambient air at the clinker cooler where a fraction of the heat is recovered at the secondary and tertiary air streams for kiln and calciner combustion respectively, and the air excess is exhaust to the environment or to other processes where heat is recovered. Figure 1 shows a schematic configuration of a five stages in-line calciner kiln, which includes a suspension preheater (SP) tower, a calciner, a rotary kiln and a clinker cooler. The SP tower consists of a cascade arrangement of cyclones.

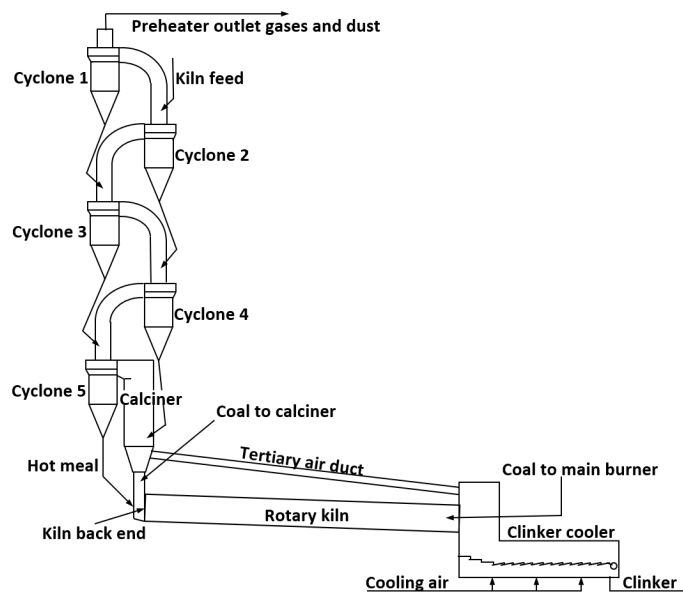


Figure 1: Five stages in-line calciner kiln

There are numerous work in energy optimization in clinker manufacturing, mainly in the clinker cooler [3, 4, 5, 6, 7], clinkerization [8, 9, 10, 11, 12, 13], cyclones' efficiency [14, 15, 16, 17] and the calcination process [18, 19, 20, 21, 22, 23, 24, 25]. An estimated reduction between 3 to 12 kcal/kg of clinker in the specific heat consumption has been reported by optimizing the kiln seals maintenance routine [26, 27, 28]. Hasanbeigi et al. [29] reported 12 kcal/kg savings by optimizing or upgrading the clinker cooler and 9 kcal/kg savings by modifying the clinker cooler with mechanical flow regulator valves to control under grate air distribution. Most of the works on the

literature that uses models for energy optimization in clinker manufacturing, consider only a small set of input variables (i.e. less than 3 input variables in most cases and only a couple of cases up to 7) for studying their effect on few response variables, mainly as a direct sensitivity analysis of one variable each time. In this work, the effect of 19 process variables (e.g. oxygen concentration in kiln and calciner, clinker bed height in clinker cooler, calciner's control temperature, etc.) was studied on 10 response variables, by simulation with Aspen Plus, and metamodels obtained by design of computer experiments [30] is reported. To the best of our knowledge this has not been reported previously in the open literature.

A simulation of a rotary kiln with five stages preheater for a Portland clinker production of 2000 t/day is implemented in this work. The simulations results are used to obtain a simplified metamodel for the process's specific heat consumption in order to (i) find the most significant process variables to minimize specific heat consumption, (ii) assess the specific heat consumption (SHC) sensitivity to changes in the process variables in a fast and efficient manner, and (iii) pinpoint process optimization opportunities in plant operation. The overall goal of this work is to evaluate the impacts in specific heat consumption for some of the main variables in the process, such as, kiln feed moisture, calciner temperature, kiln inlet gases temperature, kiln and calciner oxygen concentration, false air through kiln seals and preheater tower, cooling air, clinker bed in cooler and preheater cyclones efficiency. Additional to SHC, other 9 response variables (dust generation in the preheater tower, clinker cooler's normalized efficiency, heat losses in the preheater exit gases, secondary and tertiary air temperatures, and others) were also studied and a metamodel for each one of them was obtained and presented.

2 Simulation description

Simulations were performed using Aspen Plus V9 and consider complete heat transfer in the operation units. In an actual process, the heat transfer will be lower due to heat losses because of incomplete heat transfer.

The only fuel used in this model was coal and its combustion process was modeled based on the work by Zhang et al. [31] and Raman et al. [32]. Coal properties were specified according to plant data [33] and entered in Aspen Plus as shown in Table 1. SOLIDS property method was used for simulation for coal processing and PENG-ROB method for gas species interactions due to the high temperatures in process. Radiation and convection losses were set constant in the cooler, rotary kiln, tertiary air duct, calciner, and each cyclone, at specific values for all simulations maintaining a daily production of clinker of about 2000 metric tons per day and no significant variations were expected in process equipment external wall temperatures. This is consistent with factual plant data.

Table 1: Coal properties used as input for Aspen Plus simulations

Proximate analysis	[%]	Ultimate analysis	[%]	Sulfur analysis	[%]
Moisture	1	Carbon	68.00	Pyritic	0.4
Fix carbon	49	Hydrogen	4.00	Sulfate	0.2
Volatile matter	37	Nitrogen	1.30	Organic	0.6
Ash	14	Sulfur	1.20		
		Oxygen	11.46		
Heating value	[kcal/kg]	Chlorine	0.04		
HHV	6700	Ash	14.00		

Characterization of coal used as fuel in the process in the calciner and the kiln burner

Coal was fed to a constant pressure and temperature RYield reactor for its decomposition into its constituents in the ultimate analysis: H_2 , H_2O , N_2 , S , Cl_2 , O_2 and ashes. The heat released and the decomposition components were fed to an RGibbs reactor to simulate their most oxidized combustion products. Combustion air (air required to achieve a target of oxygen in kiln and calciner) and false air (air due to in-leaks ranging between 1% and 4% of the total gases flow) are the additional inputs for this reactor. Then, the combustion energy is used for decarbonation and clinkerization reactions in an RStoic reactor with the solids (e.g., raw meal and ashes) and combustion gases streams. This arrangement of reactors was used to model the kiln and calciner for coal's combustion and for raw materials decarbonation and clinkerization. Figure 2 shows the arrangement of reactors coupled to the suspension preheater (SP)

tower, the rotary kiln and the clinker cooler.

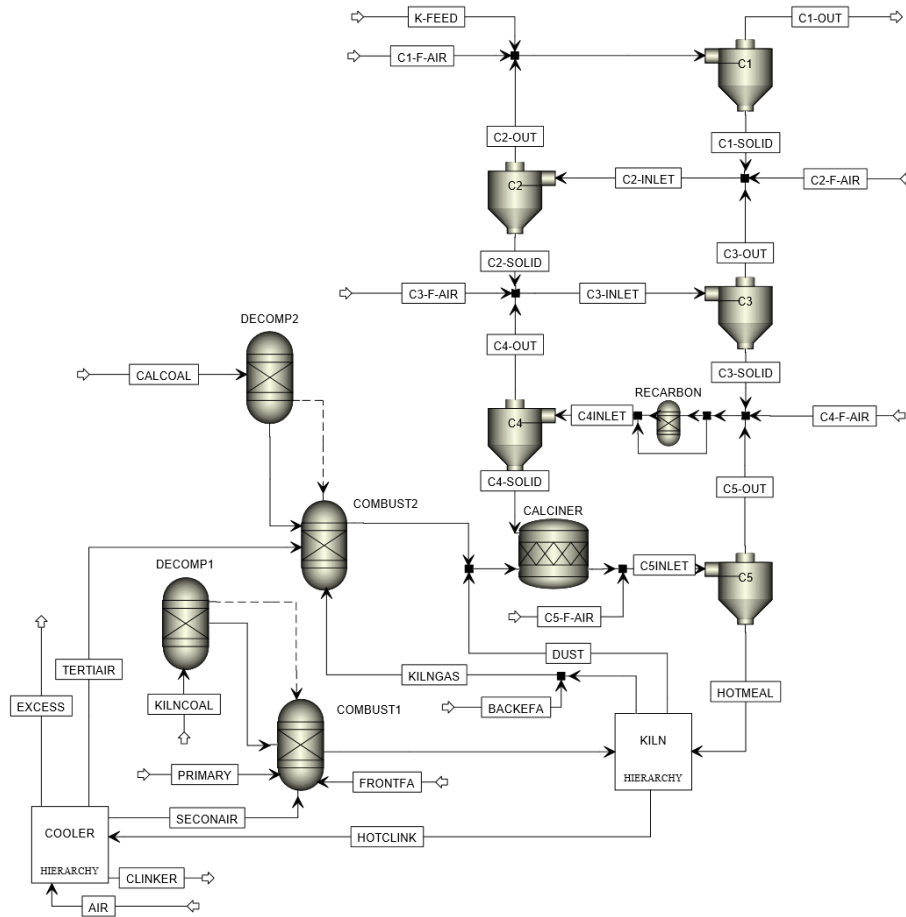


Figure 2: Aspen Plus flow diagram for preheater tower and combustion in both kiln and calciner, where, C_i is the cyclone i , for $i=1, 2, 3, 4, 5$, C_i F-AIR is the false air intake in the stage i , BACKEFA and FRONTFA are the false air intake in the kiln back end and front end, K-FEED is the kiln feed, C_i -OUT are the streams with solids and gases at cyclone i exit, KILNCOAL is the coal fed to kiln, CALCOAL is the coal fed to calciner, DECOMP1 and COMBUST1 are the RYield and RGibbs reactors for coal processing in kiln and, DECOMP2 and COMBUST 2 for calciner, PRIMARY is the air for main burner flame configuration, SECONAIR is the air from cooler to kiln (secondary air), TERTIAIR is the air from cooler to calciner (tertiary air), EXCESS is the excess air from cooler to ambient, HOTCLINK is the hot clinker from kiln to cooler and CALCINER is the RStoic reactor for calciner. The RStoic reactor for the kiln is inside the kiln hierarchy.

Limestone, chert, clay and iron ore are the main minerals used to produce the kiln feed. A roller mill is used to grind the rocks to a de-

sired particle size distribution (raw meal). The formulation of these minerals depends on the required clinker chemical composition and the fuel’s ashes and their chemical composition. The milling process was not simulated for this work. Table 2 shows the kiln feed (K-FEED) chemical composition used in this work and its experimental particle size distribution (PSD [33]). The kiln feed chemistry and PSD were set constant for the simulations.

Table 2: Experimental kiln feed composition used as input (K-FEED) for the simulation

Raw meal		Raw meal PSD			
Component	[%]	Lower limit [μm]	Upper limit [μm]	Weight fraction	Cumulative weight fraction
CaCO ₃	78.65	0.00	0.04	0.0115	0.0115
SiO ₂	13.76	0.04	0.20	0.0895	0.1010
Al ₂ O ₃	3.21	0.20	2.60	0.2044	0.3054
Fe ₂ O ₃	2.61	2.60	10.00	0.2004	0.5058
MgCO ₃	1.71	10.00	30.00	0.1913	0.6971
SO ₃	0.01	30.00	71.00	0.2020	0.8991
Na ₂ O	0.02	71.00	180.00	0.1009	1.0000

Dry basis characterization of raw meal used as kiln feed. No variations of the raw meal PSD or chemical composition were considered in the model

In the industrial operating conditions, the meal’s PSD changes through the process due to decarbonation and agglomeration of particles as the temperature increases. However, in this work PSD changes were determined by Aspen Plus only from the resulting cyclones’ separation efficiency.

Raw meal was fed to the system at the riser duct from cyclone 2 to 1 (K-FEED). The fresh feed mixes with false air (C1FA-AIR), and the dust and gases (C2-OUT) coming from stage 2 and heated until equilibrium temperature. Dust and gases are separated in cyclone 1 as per its separation efficiency (C1-OUT). A solids stream leaves cyclone 1 from the bottom (C1-SOLID) to the riser duct between stage 3 to 2 and then mixed with the dust and gases from the third cyclone’s top exit (C3-OUT) that enters cyclone 2 where it is split into gases (C2-OUT) and solids (C2-SOLID) exiting streams. This procedure is repeated along the SP tower except for the solids in

cyclone 4 (C4-SOLID) that go to calciner and the solids in cyclone 5 (HOTMEAL) that feed the rotary kiln.

All riser ducts were modeled as mixer blocks. False air was fed to those mixers. It is considered a perfect mixing and complete heat exchange between gases and solids in the mixer blocks. An RGibbs reactor was placed in a by-pass stream between the mixer from cyclone 5 to cyclone 4, where 25% of the material goes through this reactor to simulate the recarbonation process. Calciner’s decarbonation was estimated as a function of calciner’s temperature using plant’s database information and fed to the simulation model. The hot material (HOTMEAL) leaving preheater tower’s bottom stage, is fed to the rotary kiln where decarbonation is completed and clinkerization reactions take place to produce clinker.

In this work the kiln riser temperature or kiln’s back end temperature (T_{KBE}) range from 1000°C to 1100°C (literature values range of 951°C to 1100°C [23, 34, 35, 36]). The hot clinker leaves the rotary kiln at around 1400°C (previous works point to a range of 1300°C to 1400°C [36, 12, 3, 37]) and is cooled down by air in a clinker cooler as shown the figure 3.

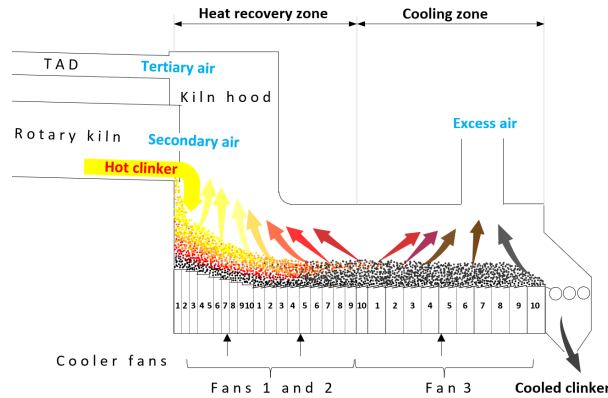


Figure 3: Cooler’s diagram of the cooling air and its distribution across the clinker bed to split itself into secondary, tertiary and excess air

The clinker stream was split into two streams to simulate the clinker bed over the cooler grates and the heat transfer between air and clinker. The cooling air flow passes first through one of the two streams and then through the other one.

In the industrial process used as reference, the clinker cooler has eight fans as sources of cooling air. To simplify the model in Aspen Plus, the eight fans were replaced by three hypothetical fans: two for the heat recovery zone for secondary air (fan 1) and tertiary air (fan 2) for combustion at the kiln and calciner respectively, and one for the cooling zone for the cooler's excess air not used in combustion (fan 3 or cooling zone fan). Secondary air goes from the cooler directly to the kiln. Tertiary air goes to the calciner through the tertiary air duct (TAD).

The cooling air from each hypothetical fan was divided into 10 streams of equal mass flow using a FSPLIT block in Aspen Plus with a fraction of 0.1 for each one (see number 1 to 10 for each fan in figure 3. In a cross current arrangement, the air exchanges heat with the clinker. As the clinker advances in the cooler it is progressively cooled down with those separate streams of cooling air. The air near the cooler discharge is exhausted from the process. The figure 4 shows a schematic configuration of the clinker cooling in aspen plus.

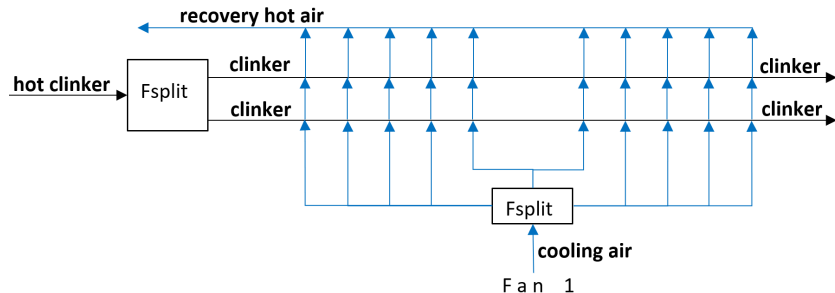


Figure 4: Clinker cooling process in Aspen Plus. The clinker splits into two streams and the cooling air into ten streams for each fan. The cooling air streams crosses in series the two clinker layers during the cooling process. This figure shows the fan 1 arrangement. The clinker leaving this process is cooled down by air from the fan 2 and then by the air from the fan 3 before leaving the clinker cooler.

Secondary and tertiary air are both drafted by the kiln induced draft fan (Kiln ID Fan) from the heat recovery zone in the clinker cooler. The two hot air streams were split after the clinker cooler (kiln hood in figure 3 with a small temperature difference approach by fixing the tertiary air to 50°C below the temperature of the secondary

air. Previous studies show the secondary air temperature ranges between 850°C and 1193°C [12, 11, 3, 38, 22, 5, 6], and the tertiary air temperature ranges from 650°C to 990°C [38, 22, 5, 6]). These reports agree with factual plant data [33].

The 19 variables studied as part of the model input are shown as in table 3. The main response variable of the model is the specific heat consumption of clinker (SHC). Other response variables are: (1) the relative power used for kiln and main filter fans ($Fan's_{\%pow}$); (2) the dust generation in the preheater tower (CKD); (3) clinker cooler normalized efficiency ($\eta_{0,8}$); (4) heat losses in the preheater exit gases (PH_{loss}), and (5) its temperature (T_{PHE}); (6) temperature of the cooler excess gases (T_{excess}); (7) the normalized volume of gases of the preheater tower per ton of clinker (G_{PH}/clk); and (8) the secondary (T_{sec}) and (9) tertiary (T_{tert}) air temperatures.

2.1 Design specifications

An important element in the simulation in Aspen Plus is the Design Spec (design specification). This is a way to add feedback controls to the simulation model. Thus, a value for a response variable can be set to manipulate one or more input variables until the desired value for the response variable is achieved. The model includes four main design specifications: two of them for combustion control in the kiln and calciner and the other two for temperature control in kiln's burning zone and calciner exit gases. The design specifications used in the process are:

- 1. Kiln oxygen mole fraction ($O_{2,kiln}$)** controlled by secondary air flow used for combustion in the kiln, that is, if a higher mole fraction of oxygen is required at the kiln back end, the secondary air supply is increased. Values used for simulations are between 1% vol. and 5% vol.

- 2. Calciner oxygen molar fraction ($O_{2,calc}$)** controlled by the tertiary air flow used for combustion in the calciner. If oxygen mole fraction required at calciner exit increases, tertiary air is increased. Values in the range of 1% to 3% were used.

3. Kiln’s burning zone temperature (T_{KBZ}) controlled by coal mass flowrate to the main burner, such that, if a higher BZT is required, coal mass flow to the kiln is increased. Kiln’s BZT was set at 1450°C for all simulations. BZT is reported within the range 1300°C to 1589°C [39, 10, 36, 40, 13, 8, 41].

4. Calciner temperature (T_{calc}) controlled by the coal mass flow to the calciner. If a higher calciner exit temperature is required, coal mass flow to the calciner is increased. In this work the calciner’s temperature used for the simulation was in the range of 865°C and 910°C according to Plant operating values. Literature values range between 800°C and 950°C [39, 21, 23, 24, 19, 10, 34].

A database of actual plant operating conditions of 6000 data points (between 31-Dic-2019 and 23-Mar-2020 every 20 minutes) was used for validation of the Aspen Plus model [33]. The data was screened for continuous periods longer than 30 hours of operation and with a variation coefficient (VC) of the kiln feed (kiln feed flow SD / kiln feed flow mean) lower than 2%. The criteria used for validation was by conducting simulations in Aspen Plus to keep kiln feed flow, preheater tower dust emission, oxygen content in kiln’s back end and calciner, and calciner’s control temperature, within the same average value in comparison with the actual plant data. Preheater tower profile and tertiary air duct were the output information from the model to validate it against plant data.

2.2 Design of experiments

A 20-run Plackett-Burman design of computer experiment was used for screening the 19 input process variables (see table 3): water in kiln feed (m_{moist}), false air in cyclones ($F_{\text{air,Ci}}$, $i=1$ to 5), kiln’s back end temperature (T_{KBE}), calciner exit temperature (T_{calc}), false air in kiln’s front end (F_{KFE}), false air in kiln’s back end (F_{KBE}), air flow in cooler fan 3 (m_{Fan3}), cyclones separation efficiency (η_{Ci}), oxygen volume concentration in gases at calciner exit ($O_{2,\text{calc}}$) and at kiln exit ($O_{2,\text{kiln}}$) and relative clinker bed height at the clinker cooler ($H_{\text{clk,bed}}$). The response variables were: process specific heat consumption (SHC), relative kiln and bag filter

fan power ($F_{\text{fan}} \text{ s}_{\%kW}$), dust escaping from preheater or cement kiln dust generation (CKD), cooler efficiency normalized at 0.8 Nm^3 of cooling air per kg of clinker ($\eta_{0.8}$), preheater losses in gases exiting the tower (PH_{loss}), temperature of gases leaving the preheater tower (T_{PHE}), temperature of excess air in the cooler (T_{excess}), ratio between normalized volume of process gases leaving the preheater tower and clinker production (G_{PH}/clk) and temperatures of secondary (T_{sec}) and tertiary air (T_{tert}).

In the actual industrial process, most of the set points for controlling the input variables are adjusted manually either directly or indirectly at the control room, e.g., raw meal moisture (m_{moist}) and fineness, fans speed or valves position, fuel dosage, oxygen levels ($O_{2,\text{calc}}$ and $O_{2,\text{kiln}}$), material bed height in clinker cooler ($H_{\text{clk,bed}}$) (or under-grate pressure) and calciner temperature (T_{calc}). However, some of the 19 variables must be modified during daily operation or maintenance, e.g., air in-leakage in all system ($F_{\text{air,C1}}$ to $F_{\text{air,C5}}$, $F_{\text{air,KFE}}$ and $F_{\text{air,KBE}}$) or cyclones' efficiency changes by modifying their geometry (η_{C1} to η_{C5}).

Table 3: 20-run Plackett-Burman experiment desing matrix and input variables

Run	m_{moist}	$F_{air,C1}$	$F_{air,C2}$	$F_{air,C3}$	$F_{air,C4}$	$F_{air,C5}$	T_{KBE}	T_{calc}	$F_{air,KFE}$	$F_{air,KBE}$	m_{Fan3}	η_{C1}	η_{C2}	η_{C3}	η_{C4}	η_{C5}	$O_{2,calc}$	$O_{2,kiln}$	$H_{clk,bed}$
1	1	1	1	1	1	1	1	1	1	1	1	1	1	1	1	1	1	1	1
2	-1	1	-1	-1	1	1	1	1	-1	1	-1	1	-1	-1	-1	-1	1	1	-1
3	-1	-1	1	-1	-1	1	1	1	1	-1	1	-1	1	-1	-1	-1	-1	1	1
4	1	-1	-1	1	-1	-1	1	1	1	1	-1	1	-1	1	-1	-1	-1	-1	1
5	1	1	-1	-1	1	-1	-1	1	1	1	1	-1	1	-1	1	-1	-1	-1	-1
6	-1	1	1	-1	-1	1	-1	-1	1	1	1	1	-1	1	-1	1	-1	-1	-1
7	-1	-1	1	1	-1	-1	1	-1	-1	1	1	1	1	-1	1	1	-1	-1	-1
8	-1	-1	-1	1	1	-1	-1	-1	-1	-1	1	1	1	1	-1	1	-1	1	-1
9	-1	-1	-1	-1	1	1	-1	-1	-1	-1	1	1	1	1	1	-1	1	-1	1
10	1	-1	-1	-1	-1	1	1	-1	-1	-1	-1	-1	1	1	1	1	-1	1	-1
11	-1	1	-1	-1	-1	-1	1	1	-1	-1	1	-1	-1	1	1	1	1	-1	1
12	1	-1	1	-1	-1	-1	-1	1	1	-1	-1	1	-1	-1	1	1	1	1	-1
13	-1	1	-1	1	-1	-1	-1	-1	1	1	-1	-1	1	-1	-1	1	1	1	1
14	1	-1	1	-1	1	-1	-1	-1	-1	1	1	-1	-1	1	-1	-1	1	1	1
15	1	1	-1	1	-1	1	-1	-1	-1	-1	1	1	-1	-1	1	-1	-1	1	1
16	1	1	1	-1	1	-1	1	-1	-1	-1	1	1	-1	-1	1	-1	-1	-1	1
17	1	1	1	1	-1	1	-1	1	-1	-1	-1	-1	1	1	-1	-1	1	-1	-1
18	-1	1	1	1	1	-1	1	-1	1	-1	-1	-1	-1	1	1	-1	-1	1	-1
19	-1	-1	1	1	1	1	-1	1	-1	1	-1	-1	-1	-1	1	1	-1	-1	1
20	1	-1	-1	1	1	1	1	-1	1	-1	1	-1	-1	-1	-1	1	1	-1	-1

Factor	Input variable	Coded level		Factor	Input variable	Coded Level	
		-1	1			-1	1
m_{moist} :	Water in kiln feed (kg/h)	254	1022	m_{Fan3} :	Cooler fan 3 (kg/h)	46340	67756
$F_{air,C1}$:	Cyclone 1 false air (kg/h)	1521	6482	η_{C1} :	Cyclone 1 efficiency (%)	89	94
$F_{air,C2}$:	Cyclone 2 false air (kg/h)	1521	6482	η_{C2} :	Cyclone 2 efficiency (%)	85	90
$F_{air,C3}$:	Cyclone 3 false air (kg/h)	1521	6482	η_{C3} :	Cyclone 3 efficiency (%)	80	85
$F_{air,C4}$:	Cyclone 4 false air (kg/h)	1521	6482	η_{C4} :	Cyclone 4 efficiency (%)	80	85
$F_{air,C5}$:	Cyclone 5 false air (kg/h)	1521	6482	η_{C5} :	Cyclone 5 efficiency (%)	75	80
T_{KBE} :	Kiln back end temperature ($^{\circ}$ C)	1000	1100	$O_{2,calc}$:	Calciner's exit oxygen (% vol)	1	3
T_{calc} :	Calciner temperature ($^{\circ}$ C)	865	910	$O_{2,kiln}$:	Kiln's exit oxygen (% vol)	1	5
$F_{air,KFE}$:	Kiln's front end false air (kg/h)	369	1843	$H_{clk,bed}$:	Relative clinker height (%)	50	100
$F_{air,KBE}$:	Kiln's back end false air (kg/h)	369	1843				

Factors are the input variables for the Aspen Plus simulations.

All 19 variables were set with minimum (-1) and maximum (+1) coded levels for simulation in Aspen Plus per the 20-run Plackett-Burman design described. Levels for input variables were determined according to historical or feasible process values (see table 3). The results were analyzed with R's BsMD [42] package and then, linear metamodells were constructed with the input variables having the highest posterior probabilities on the dependent variables and using the same runs from the Plackett-Burman design by performing multivariate linear regressions. Due to its large overall impact, the specific heat consumption (SHC) metamodel, as a function of the input variables with the highest significance, was minimized by setting up a constrained linear programming optimization problem and solving it with GAMS [43] using CONOPT's solver [44]. A new 20-run Plackett-Burman was simulated in Aspen Plus but keeping constant the input variables at their optimum values pursuing a minimized SHC to verify that (i) the discarded input variables in SHC metamodel were not statistically influential and (ii) the ranges

of operation for the optimum SHC.

The input variables with the highest significance on SHC were used to perform a relative sensitivity analysis simulation in Aspen Plus and with the metamodel. Relative sensitivity (see equation 1) provides information about the impact of the fractional increment of a variable or a parameter on the fractional increment of response variable and, since sensitivities are non-dimensional, their values can be cross-compared to find where should process optimization efforts be directed.

$$S_{X_i}^{f(\vec{X})} = \frac{\overline{X_i} \Delta f(\vec{X})}{f(\vec{X}) \Delta X_i}, \quad (1)$$

Where, X_i is one of the 19 input variables, $f(\vec{X})$ is the linear metamodel for the response variables, $S_{X_i}^{f(\vec{X})}$ is the relative sensitivity of $f(\vec{X})$ with respect to X_i , $\overline{X_i}$ is the average value of X_i on the evaluation range, $\overline{f(\vec{X})}$ is the average value of $f(\vec{X})$ on the evaluation interval and ΔX_i is a small change in X_i that produces a change $\Delta f(\vec{X})$ for the response variable $f(\vec{X})$.

Comparisons of sensitivities between the simulation in Aspen and the metamodel amount to double-checking how good the metamodels fit simulation results and dealing with possible curvature in the factual process data.

3 Results and discussion

Aspen Plus model validation

Five periods of kiln stable running operation were averaged [33] and each one of those periods were used as inputs to five different simulations. A summary of the plant and simulation results is shown in table 4.

Table 4: Plant actual data and simulation results comparison for optimal conditions

Variable	Units	Plant data			Simulation			Confidence interval	
		μ_1	\pm	SD	μ_2	\pm	SD	$\mu_1 - \mu_2$	$1-\alpha = 0.95$
T_{C1}	$^{\circ}\text{C}$	334	\pm	9	327	\pm	6	(-1.2 , 15.2)	
T_{C2}	$^{\circ}\text{C}$	490	\pm	10	512	\pm	7	(-31.1 , -12.9)	
T_{C3}	$^{\circ}\text{C}$	656	\pm	5	652	\pm	7	(-0.6 , 8.6)	
T_{C4}	$^{\circ}\text{C}$	820	\pm	3	778	\pm	4	(39.3 , 44.7)	
T_{C5}	$^{\circ}\text{C}$	907	\pm	4	905	\pm	0	(-1.2 , 6.0)	
T_{TAD}	$^{\circ}\text{C}$	857	\pm	26	878	\pm	19	(-44.7 , 2.7)	
$O_{2,\text{kiln}}$	mol%	4.17	\pm	1.40	4.25	\pm	0.23	(-1.4 , 1.2)	
O_2 PHE	mol%	3.09	\pm	0.49	3.03	\pm	0.38	(-0.4 , 0.5)	

T_{Ci} is the temperature of the cyclone C_i (for $i=1$ to 5) in the preheater tower, T_{TAD} is the temperature at the tertiary air duct, $O_{2,\text{kiln}}$ is the volume oxygen concentration in kiln's back end and O_2 PHE is the volume oxygen concentration in the preheater exit. The input variables for the Aspen Plus simulation were kiln feed, kiln's back end and calciner oxygen concentration and calciner's control temperature (T_{C5}). Validation variables were the preheater temperature profile at each cyclone exit. The confidence interval is shown for each variable. μ_1 is the average of plant data and μ_2 the average of simulation results

All the variables compared except for the temperatures of cyclones 2 and 4 show that there are no significant differences between plant data and the simulation using a 95% confidence interval (CI). For the T_{C2} the CI shows that $\mu_1 < \mu_2$ because both endpoints are negative and the simulation is over-predicting the exit temperature by at least 13°C which represents a 2% deviation with respect to plant data. For cyclone 4 the CI shows that $\mu_1 > \mu_2$ (a positive difference), therefore the simulation under-predicts T_{C4} . The deviation in this case is at least 39°C and represents a 4% deviation with respect to plant data.

Considering in-leakage air or recarbonation differences between simulations and actual plant conditions the model consistently reproduces very well plant data conditions. The small temperature differences in T_{C2} and T_{C4} are within expected measurement errors and temperature profiles in the cyclones (not considered in the simulations). Moreover, since the stage 1 control volume boundaries are used for the heat balance and its process variables are within the range of plant data as well as other key variables like calciner's oxygen concentration, tertiary air temperature and calciner's control temperature this model is deemed appropriate for the purpose

of pinpointing optimization opportunities in the process.

Metamodel for calculation of SHC

After the simulation of the runs 1 to 20 (see table 5), a mean value of 782 kcal/kg of clinker was obtained for the SHC in a range between 753 to 814 kcal/kg of clinker. Linear metamodels were constructed with the input variables having the highest posterior probabilities on the dependent variables. The metamodel for the specific heat consumption (SHC) was found to be driven by false air in cyclones 4 ($F_{\text{air,C4}}$) and 5 ($F_{\text{air,C5}}$), cooler clinker bed depth ($H_{\text{clk,bed}}$), target oxygen in calciner ($O_{2,\text{calc}}$) and calciner operating temperature (T_{calc}). Although other variables affected the SHC, they were not considered in the model due to their low significance. The metamodel for SHC is shown in equation 2. This implies that efforts in minimizing the specific heat optimization should focus on these variables. Though, these efforts need further confirmation by performing process optimization runs in daily operations.

$$\text{SHC} = 781.89 + 3.67 \cdot F_{\text{air,C4}} + 3.28 \cdot F_{\text{air,C5}} + 4.16 \cdot T_{\text{calc}} + 9.16 \cdot O_{2,\text{calc}} - 12.70 \cdot H_{\text{clk,bed}} \quad (2)$$

The mean absolute error of the SHC for the metamodel compared to the simulations was 2.3 kcal/kg clinker and the maximum absolute error was 5.3 kcal/kg clinker. The SHC metamodel was validated against the Aspen Plus model using values of 30% and 70% of the input variables in a similar Plackett-Burman matrix (runs 41 to 60). In this case, the mean absolute error of the metamodel was 2.8 kcal/kg clinker and the maximum absolute error 7.2 kcal/kg clinker, 29% and 74% of the range for SHC simulation results, respectively. This represents a very good fit for a highly simplified linear metamodel ($R^2=0.9643$) compared to the complexity of the Aspen Plus model. The SHC metamodel can be used for quick estimations about the impact in the SHC when changing the input variables and should prove most valuable for plant operations.

Optimization of the SHC

The obtained metamodel (equation 2) was used to optimize the input variables with the highest impact in SHC, except that the calciner’s temperature (T_{calc}) was fixed at (887.5°C) and not at its minimum value (865°C), because this value is more consistent with process data for industrial clinker calciners. The optimization was not performed directly in Aspen Plus as it would require manipulating simultaneously 19 input variables.

Runs 21 to 40 (see table 5) use the same parameters as in the previous 20 runs but keeping constant $F_{\text{air},C4} = 1,521 \text{ kg/h}$ (cyclone 4 false air), $F_{\text{air},C5} = 1,521 \text{ kg/h}$ (cyclone 5 false air), $T_{\text{calc}} = 887.5^{\circ}\text{C}$ (calciner’s control temperature), $O_{2,\text{calc}} = 1\% \text{ vol}$ (O_2 at calciner outlet) and $H_{\text{clk,bed}} = 100\%$ (relative clinker height in the cooler) to minimize SHC. A SHC between $747.5 - 758.1 \text{ kcal/kg}$ of clinker was found for the optimized scenarios, with a mean of 753 kcal/kg , which is 29 kcal/kg of clinker lower than the mean of the first round of simulations (782 kcal/kg). Moreover, nine out of ten response variables had a lower standard deviation (SD) in the optimized scenario (e.g., the SD of the temperature of the cooler exit gases dropped a 62% from 64K to 24K and the SD of the normalized cooler efficiency dropped 92% from 3.1% to 0.3%), indicating a most stable process with only $\pm 3 \text{ kcal/kg}$ of clinker in the standard deviation of the SHC. In this case the main fans’ power were found in the range of 60% to 70% of the initial maximum value and 15% less power consumption on average.

Table 5 shows the results of all the response variables obtained in the simulation in both the first 20 runs and optimized SHC runs 21 to 40, using the Plackett-Burman experimental design.

The only response variable that did not reduced its standard deviation after the optimization was the cement kiln dust (CKD) generation. This variable depends mostly on the cyclones’ separation efficiency, and thus, it did not change with the optimization process. All other response variables were optimized indirectly on its mean value (reduction in heat losses or energy consumption and increasing in heat recovery), except for the temperature of excess air in the cooler which increased by $\text{ca.}1^{\circ}\text{C}$ (higher losses). This increase in temperature is explained by a lower cooling air mass flow due the SHC reduction and a small increase in clinker temperature (5°C ,

Table 5: 20-run Plackett-Burman experiment desing results for first and optimized rounds

Response variables	Runs 1 - 20 Aspen Plus			Runs 21 - 40 (optimized round) Aspen Plus			Metamodels			Metamodels abs. error	
	mean	±	SD	mean	±	SD	mean	±	SD	mean	max
SHC, (kcal/kg clinker)	782	±	17	753	±	3	753	±	0	3	6
Fan's _{pow} , (%)	80.0	±	12	65.1	±	2	64	±	2	2	4
CKD, (t/h)	10.4	±	3.1	10.4	±	3.1	10.4	±	3.1	0.2	0.5
$\eta_{0,8}$, (%)	66.9	±	3.2	70.8	±	0.3	70.7	±	0.0	0.22	0.49
PH _{losses} , (kcal/kg clinker)	201	±	23	171	±	3	170	±	2	2	5
T _{PHE} , (°C)	317	±	22	292	±	7	292	±	7	2	5
T _{excess} , (°C)	292	±	64	293	±	24	293	±	23	5	10
G _{PH/clk} , (Nm ³ /kg clinker)	1.56	±	0.13	1.40	±	0.05	1.40	±	0.05	0.00	0.01
T _{sec} , (°C)	902	±	68	990	±	6	983	±	0	7	15
T _{tert} , (°C)	852	±	68	940	±	6	933	±	0	7	15

Cooler efficiency results in this table were normalized to a combustion air recovery from cooler to the process of 0.8 Nm³/kg clinker. Where: SHC is the specific heat consumption; Fan's_{pow} is the relative kiln and bag filter fans power; CKD is the cement kiln dust generation; $\eta_{0,8}$ is the normalized cooler efficiency; PH_{losses} is the preheater losses in gases; T_{PHE} is the Preheater exit gases temperature; T_{excess} is the cooler excess gases temperature; G_{PH/clk} is the ratio PH gases to clinker; T_{sec} is the secondary ai temperature and T_{tert} is the tertiary air temperature.

from 149°C to 154°C).

Changes of 5% in cyclones' dust collection efficiency (η_{Ci} , for i=1 to 5) and oxygen concentration in kiln's back end ($O_{2,kiln}$) were found not significant for the SHC. Also, oxygen concentration in kiln back end and false air in kiln and in cyclones 1, 2 and 3 had no significant impact in the SHC within the analyzed range of input variables.

A summary of the results of mean value, standard deviation, mean absolute error and maximum absolute error are presented in table 5 for each metamodel . Considering the initial standard deviation, in runs 21 to 40, all variables presented a mean absolute error (MAE) similar to the standard deviation for most of the response variables. The maximum absolute error double the MAE (e.g. 2.3 times in average).

Linear metamodels

For each dependent variable a metamodel of the form

$$\hat{Y}_j = \beta_{0-j} + \sum_i \beta_{i-j} X_i$$

was constructed with the factors that had the largest marginal posterior probability, where \hat{Y}_j is a predicted response variable, β_{0-j}

and β_{i-j} are fitted parameters and X_i are the most significant input variables as per the Bayes Discrimination Model. The same matrix for the Plackett-Burman design of experiment was used. This allowed to construct all of the metamodels required.

The formulas that represent the remaining metamodels are:

$$\begin{aligned} \text{Fan}'s_{\%pow} = & 80.01 + 1.84F_{\text{air,C3}} + 2.58F_{\text{air,C4}} + 1.78T_{\text{calc}} \\ & + 10.97O_{2,\text{calc}} - 2.13H_{\text{clk,bed}}, \quad R^2 = 0.9496 \quad (3) \end{aligned}$$

$$\text{CKD} = 10.42 - 3.081\eta_{C1} - 0.514\eta_{C2}, \quad R^2 = 0.9949 \quad (4)$$

$$\eta_{0.8} = 66.86 - 0.81O_{2,\text{calc}} + 3.08H_{\text{clk,bed}}, \quad R^2 = 0.9734 \quad (5)$$

$$\begin{aligned} \text{PH}_{\text{losses}} = & 201.0 + 2.38F_{\text{air,C3}} + 4.57F_{\text{air,C4}} + 4.87T_{\text{calc}} + 21.66O_{2,\text{calc}} \\ & - 4.39H_{\text{clk,bed}}, \quad R^2 = 0.9849 \quad (6) \end{aligned}$$

$$\begin{aligned} T_{\text{PHE}} = & 317.3 - 4.38m_{\text{moist}} - 2.60F_{\text{air,C1}} + 3.06F_{\text{air,C4}} + 6.72T_{\text{calc}} \\ & + 5.04\eta_{C1} + 18.79O_{2,\text{calc}} - 3.67H_{\text{clk,bed}}, \quad R^2 = 0.9946 \quad (7) \end{aligned}$$

$$\begin{aligned} T_{\text{excess}} = & 292.4 + 10.69F_{\text{air,C5}} - 23.18m_{\text{Fan3}} - 46.43O_{2,\text{calc}} \\ & - 34.66H_{\text{clk,bed}}, \quad R^2 = 0.981 \quad (8) \end{aligned}$$

$$\begin{aligned} G_{\text{PH}/\text{clk}} = & 1.561 + 0.026F_{\text{air,C1}} + 0.027F_{\text{air,C2}} + 0.029F_{\text{air,C3}} \\ & + 0.032F_{\text{air,C4}} + 0.111O_{2,\text{calc}} - 0.018 \cdot H_{\text{clk,bed}} \\ & R^2 = 0.9988 \quad (9) \end{aligned}$$

$$\begin{aligned} T_{\text{sec}} = & 902.3 + 12.3F_{\text{air,C5}} - 49.2O_{2,\text{calc}} + 43.8H_{\text{clk,bed}} \\ & R^2 = 0.9777 \quad (10) \end{aligned}$$

$$\begin{aligned} T_{\text{tert}} = & 852.3 + 12.3F_{\text{air,C5}} - 49.2O_{2,\text{calc}} + 43.8H_{\text{clk,bed}} \\ & R^2 = 0.9777 \quad (11) \end{aligned}$$

Although metamodels were obtained from the results of the Aspen Plus simulations in the first round of Plackett-Burman experiments, results for optimized scenario show a very good fit despite the fact that they are very simple models compared to the Aspen Plus simulation. Moreover, these models can be used independent of the simulation software to obtain adequate estimates of the process behavior. Those models can be used to have an idea about magnitude and direction of the impact of one or several input variables on the specific metamodel response variable. It is important to state that input values for the metamodels are restricted to the range of the coded levels (-1 to +1) and are not to be extrapolated because of statistical estimation problems.

The figure 5 shows the box and whisker plot for the response variables in the optimized scenario. Black bars are the Aspen Plus results for runs 21-40 and white bars are linear metamodels results.

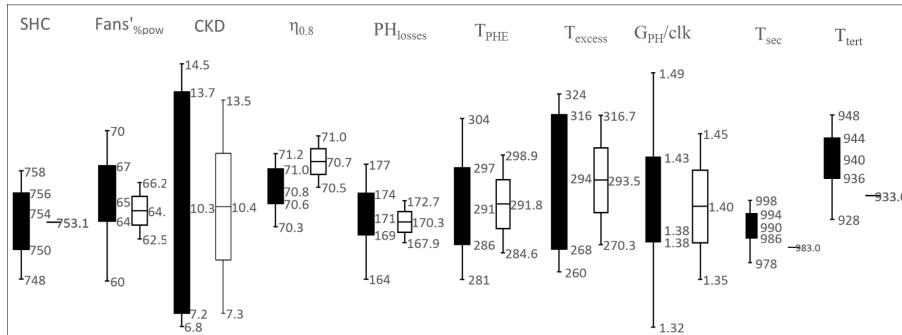


Figure 5: Box and whisker plot of Aspen Plus (black bars) and Metamodels (white bars) in the optimized scenario. Vertical axis is not scale to compare different response variables. Coded levels for the constant factors were: -1, -1, -1, 0 and 1 for $F_{air,C4}$, $F_{air,C5}$, $O_{2,calc}$, T_{calc} and $H_{clk,bed}$, respectively.

Notice that SHC, T_{sec} and T_{tert} are constant values, because these response variables depend exclusively from one or more of the constant factors ($F_{air,C4}$, $F_{air,C5}$, $O_{2,calc}$, T_{calc} and $H_{clk,bed}$). All the metamodels results match in the same range or in a fraction in comparison with Aspen Plus results and are according to the maximum absolute error and the MAE in table 5.

Sensitivity analysis for the SHC

After the SHC was optimized using the metamodel, a sensitivity analysis in Aspen Plus and the metamodel were carried out for each input variable in the SHC metamodel (that is, $F_{\text{air,C4}}$, $F_{\text{air,C5}}$, T_{calc} , $O_{2,\text{calc}}$ and $H_{\text{clk,bed}}$) to estimate their individual relative impacts on the SHC for the process. All of the analysis simulation were performed with the Plackett-Burman run 30 conditions in the optimized scenario. The relative sensitivity was calculated with equation 1 and the results are shown in figure 6.

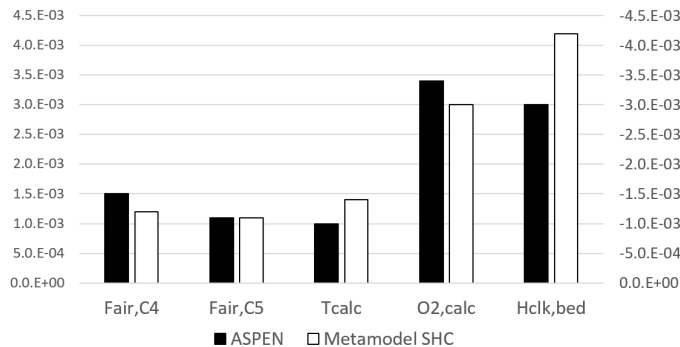


Figure 6: Relative sensitivity analysis results for the SHC. Input factors were set constant according to run 30 in combination with the minimized input variables of the equation 2. Relative sensitivity of the SHC due changes in $H_{\text{clk,bed}}$ is negative (right axis) and other factors are positives and shown in the left axis. Coded levels used for evaluation were 0 and 0.5, then $\Delta X_i = 0.5$ and $\bar{X}_i = 0.25$.

As the SHC metamodel was obtained from the Aspen Plus results using the maximum and minimum values of the input variables, this analysis allowed to compare the relative sensitivity of each input variable on the SHC within the range for the SHC metamodel and the Aspen Plus model. Results are consistent (both are in the same order of magnitude) despite the non-linear nature of the Aspen Plus model against the highly simplified linear SHC metamodel. The most significant input variables per the relative sensibility analysis are the clinker bed height and oxygen concentration at calciner exit followed by the calciner’s control temperature. False air in cyclones 4 and 5 have a secondary impact on the SHC. Therefore, optimizing clinker cooler operation and minimizing oxygen at calciner outlet should be one of the main tasks for SHC optimization, followed by minimizing calciner’s control temperature and reducing the false air in-leakage.

Linear metamodels validation

Despite the excellent agreement among the metamodels, the Aspen Plus simulation and the plant’s data at the fitting points, it is important to address possible curvature issues in the metamodels. Thus, 20 additional simulations (runs 41 to 60) were performed with Aspen Plus using intermediate values corresponding to 30% and 70% of the range used in the original fitting (i.e., the coded values were set at -0.4 and 0.4). A summary of the results of the validation of curvature issues are presented in table 6.

Table 6: Validation of metamodels. Simulation runs 41 to 60

Response variable	Units	Aspen Plus			Metamodels			Abs. error	
		mean	±	SD	mean	±	SD	mean	max
SHC	kcal/kg clinker	780	±	9	782	±	7	3	7
Fan’s _{pow}	%	78	±	5	80	±	5	2	3
CKD	t/h	10.1	±	1.2	10.4	±	1.2	0.3	0.7
$\eta_{0.8}$	%	67.1	±	1.7	66.9	±	1.3	0.4	1.1
PH _{losses}	kcal/kg clinker	199	±	10	201	±	9	2	5
T _{PHE}	°C	317	±	9	317	±	9	1	2
T _{excess}	°C	263	±	19	292	±	25	29	43
G _{PH/clk}	Nm ³ /kg clinker	1.55	±	0.05	1.56	±	0.05	0.01	0.02
T _{sec}	°C	910	±	30	902	±	27	8	21
T _{tert}	°C	860	±	30	852	±	27	8	21

Runs 41 to 60 using coded levels -0.4 and 0.4 for all 19 input variables using Plackett-Burman matrix. This represents values in 30% and 70% of the interval for each input variable. MAE is similar to the runs 21 to 40 despite of the new values used for the simulations.

These results suggest that none of the metamodels presented curvature issues (i.e., the error in these experiments is approximately equal to the previous ones with a larger range of levels for the factors) with the exception of T_{excess} (i.e. the metamodel is not appropriate to perform interpolations to predict dependent variable values at intermediate levels of the uncoded input variables.) Including the new runs into the analysis fixes the curvature problem and the new metamodel is:

$$T_{\text{excess}} = 278.0 + 9.99F_{\text{air,C5}} - 22.48m_{\text{Fan3}} - 45.25O_{2,\text{calc}} - 32.67H_{\text{clk,bed}}$$

$$R^2 = 0.9 \quad (12)$$

The mean absolute error was reduced from 29°C to 14°C which

represents an adequate fit for this response variable. We tested the corrected model against a run where all factors were set at the middle of the level range (i.e., a central run where all coded factors are now at the zero coded level). The result for T_{excess} in Aspen plus yielded 277.4°C while the corrected model predicts T_{excess} of 278°C . Thus, equation 12 replaces equation 8. Similar results are obtained with the remaining variables.

However, all other metamodels showed a good fit to the Aspen Plus model. For instance, the figure 7 shows the fit of the SHC metamodel against the Aspen Plus model.

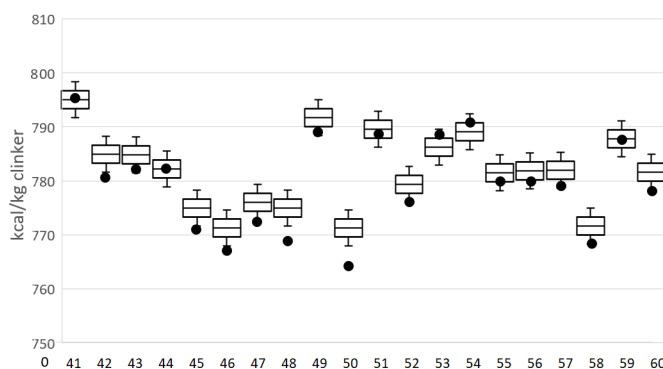


Figure 7: SHC results for runs 41 to 60 for Aspen Plus model (black circle) and SHC metamodel (white boxes). Standard error from multivariable regression for SHC metamodel is plotted as the error in the metamodel prediction.

The standard error was 3 kcal/kg of clinker and it is show in the figure 3 as the intervals for the SHC metamodel. This means that the SHC metamodel is a very good tool for estimations about the magnitude of the impact of the five input variables in equation 2 on the industrial process.

4 Conclusions and future work

A dry process cement kiln model was done in Aspen Plus V9. The model was validated with data from a 2000 metric ton per day in-line

calciner cement kiln. The simulations were validated by comparing the preheater tower temperature profile. The model used as input the kiln feed flow, chemical composition and particle size distribution, preheater cyclones geometry, calciner's control temperature (cyclone five exit gas temperature) and the oxygen levels in kiln back end and calciner outlet (cyclone five exit gas).

A 20-run Plackett-Burman design of computer experiments with 19 input variables and 10 response variables was performed using the Aspen Plus simulation to fit the response variables with the most significant input variables to simplify linear metamodels. The SHC metamodel indicated that false air in cyclones 4 and 5, calciner's control temperature, oxygen concentration at calciner exit and cooler's clinker bed depth were the most significant input variables on SHC.

The SHC metamodel was used to minimize SHC by finding the values of the main input variables. The settings were further validated using a PB DOE keeping the optimized input variables for SHC while varying the remaining ones. Optimizing clinker cooler operation and to minimize oxygen concentration at the calciner exit should become one of the main tasks for SHC optimization, followed by minimization of calciner's temperature where the kiln operates optimally and reduction in false air in-leakage by maintenance and production efforts.

Changes of 5% in cyclones' dust collection efficiency and oxygen concentration in kiln's back end were found not significant in the SHC of the process. Also, oxygen concentration in kiln back end and false air in kiln and in cyclones 1, 2 and 3 had no significant impact in the SHC when proportions are within the analyzed range.

The SHC metamodel was minimized and the optimized values were set as constants input for a second round of Plackett-Burman runs. The SHC obtained in Aspen Plus was reduced by a mean of 29 kcal/kg of clinker (from 782 kcal/kg clinker to 753 kcal/kg clinker) by setting constant $F_{\text{air,C4}}$ in 1521 kg/h, $F_{\text{air,C5}}$ in 1% 1521kg/h, T_{calc} in 887.5°C, $O_{2,\text{calc}}$ in 1%vol and $H_{\text{clk,bed}}$ in 100% (the coded levels were set at -1, -1, 0, -1 and 1, respectively) . This metamodel can be used as a guideline of the main points to optimize in the cement plant to reduce specific heat consumption, which in some

cases might be obvious for cement engineers, but as the model discards other variables, it reduces the number of distractors affecting this key indicator and enabling to focus on the daily most important tasks to optimize the SHC.

A sensitivity analysis was conducted with both, Aspen Plus simulations and the SCH metamodel. The relative sensitivity was calculated for each of the SHC metamodel variables ($F_{\text{air,C4}}$, $F_{\text{air,C5}}$, $O_{2,\text{calc}}$ and $H_{\text{clk,bed}}$). With this analysis, the two most impacting variables were found to be the oxygen concentration at calciner's outlet and the cooler's clinker bed deepness. The other three variables (false air in cyclones 4 and 5 and calciner's control temperature) were in the same range of impacting the heat consumption.

On another hand, the SHC metamodel presented a mean absolute error of 3 kcal/kg of clinker and a maximum of 7 kcal/kg of clinker in runs 21 to 60 in comparison with Aspen Plus simulations. It should be considered that the SHC metamodel was determined from the first round of Plackett-Burman experiments. This low deviation represents a very good performance of the predictions for the metamodel and it is a very good tool for estimations about the magnitude of the impact of the five input variables: false air in cyclone 4 and 5, calciner's control temperature, oxygen concentration at calciner exit and clinker bed height in the clinker cooler.

As part of the future works derived from this thesis, a response surface methodology (RSM) design of computer experiment including intermediate values for the most significant factors can be implemented to further optimize and validate the results for the optimization and the sensitivity analysis.

References

- [1] U.S. energy information administration and department of energy. *International Energy Outlook 2019, with Projections to 2050*. Sept. 2019. URL: <https://www.eia.gov/outlooks/ieo/pdf/ieo2019.pdf>.
- [2] D. Saygin et al. "Benchmarking the energy use of energy-intensive industries in industrialized and in developing countries". In: *Energy* 36.11 (Nov. 2011), pp. 6661–6673. DOI: 10.1016/j.energy.2011.08.025.

- [3] Wei Shao, Zheng Cui, and Lin Cheng. “Multi-objective optimization design of air distribution of grate cooler by entropy generation minimization and genetic algorithm”. In: *Applied Thermal Engineering* 108 (Sept. 2016), pp. 76–83. DOI: 10.1016/j.applthermaleng.2016.07.088.
- [4] Wei Shao, Zheng Cui, and Lin Cheng. “Multi-objective optimization of cooling air distributions of grate cooler with different clinker particles diameters and air chambers by genetic algorithm”. In: *Applied Thermal Engineering* 111 (Jan. 2017), pp. 77–86. DOI: 10.1016/j.applthermaleng.2016.09.082.
- [5] Meiqi Wang et al. “Numerical Simulation and Analytical Characterization of Heat Transfer between Cement Clinker and Air in Grate Cooler”. In: *Journal of Chemical Engineering of Japan* 49.1 (2016), pp. 10–15. DOI: 10.1252/jcej.14we414.
- [6] J.U. Ahamed et al. “Assessment of energy and exergy efficiencies of a grate clinker cooling system through the optimization of its operational parameters”. In: *Energy* 46.1 (Oct. 2012), pp. 664–674. DOI: 10.1016/j.energy.2012.06.074.
- [7] Yan Wen, Yan-Xu Ju, and Lin Yuan. “Research on heat transfer law of cement clinker accumulation body in grate cooler based on lattice Boltzmann method”. In: *Heat Transfer-Asian Research* 48.1 (Oct. 2018), pp. 270–285. DOI: 10.1002/htj.21383.
- [8] Z. Liu et al. “Thermal efficiency modelling of the cement clinker manufacturing process”. In: *Journal of the Energy Institute* 88.1 (Feb. 2015), pp. 76–86. DOI: 10.1016/j.joei.2014.04.004.
- [9] K.S. Mujumdar and V.V. Ranade. “Simulation of Rotary Cement Kilns Using a One-Dimensional Model”. In: *Chemical Engineering Research and Design* 84.3 (Mar. 2006), pp. 165–177. DOI: 10.1205/cherd.04193.
- [10] Ziya Söğüt, Zuhul Oktay, and Hikmet Karakoç. “Mathematical modeling of heat recovery from a rotary kiln”. In: *Applied Thermal Engineering* 30.8-9 (June 2010), pp. 817–825. DOI: 10.1016/j.applthermaleng.2009.12.009.
- [11] Kaustubh S. Mujumdar and Vivek V. Ranade. “CFD modeling of rotary cement kilns”. In: *Asia-Pacific Journal of Chemical Engineering* 3.2 (Mar. 2008), pp. 106–118. DOI: 10.1002/apj.123.
- [12] Kaustubh S. Mujumdar et al. “Rotary Cement Kiln Simulator (RoCKS): Integrated modeling of pre-heater, calciner, kiln and clinker cooler”. In: *Chemical Engineering Science* 62.9 (May 2007), pp. 2590–2607. DOI: 10.1016/j.ces.2007.01.063.
- [13] Konrad S. Stadler, Jan Poland, and Eduardo Gallestey. “Model predictive control of a rotary cement kiln”. In: *Control Engineering Practice* 19.1 (Jan. 2011), pp. 1–9. DOI: 10.1016/j.conengprac.2010.08.004.

- [14] Elham Kashani, Ali Mohebbi, and Mahdi Ghaedi Heidari. “CFD simulation of the preheater cyclone of a cement plant and the optimization of its performance using a combination of the design of experiment and multi-gene genetic programming”. In: *Powder Technology* 327 (Mar. 2018), pp. 430–441. DOI: 10.1016/j.powtec.2017.12.091.
- [15] Francesco Mariani, Francesco Risi, and Carlo N. Grimaldi. “Separation efficiency and heat exchange optimization in a cyclone”. In: *Separation and Purification Technology* 179 (May 2017), pp. 393–402. DOI: 10.1016/j.seppur.2017.02.024.
- [16] Li Long Dong et al. “The Effect of Inner Cylinder on Cyclone Preheater Using Fluent Software”. In: *Advanced Materials Research* 1030-1032 (Sept. 2014), pp. 1352–1355. DOI: 10.4028/www.scientific.net/amr.1030-1032.1352.
- [17] Marek Wasilewski and Lakhbir Singh Brar. “Optimization of the geometry of cyclone separators used in clinker burning process: A case study”. In: *Powder Technology* 313 (May 2017), pp. 293–302. DOI: 10.1016/j.powtec.2017.03.025.
- [18] Ahmet Kolip. “Energy and exergy analyses of a serial flow four cyclone stages precalciner type cement plant”. In: *Scientific Research and Essays* 5.18 (Sept. 2010), pp. 2702–2712. ISSN: 1992-2248. URL: <http://www.academicjournals.org/SRE>.
- [19] Amila Chandra Kahawalage, Morten C Melaaen, and Lars-André Tokheim. “Numerical modeling of the calcination process in a cement kiln system”. In: *Proceedings of the 58th Conference on Simulation and Modelling (SIMS 58) Reykjavik, Iceland, September 25th – 27th 2017*. Linköping University Electronic Press, Sept. 2017. DOI: 10.3384/ecp1713883.
- [20] Jun Lin Xie and Shu Xia Mei. “Numerical Simulation of Gas-Solid Flow in a Precalciner of Cement Industry”. In: *Materials Science Forum* 575-578 (Apr. 2008), pp. 1234–1239. DOI: 10.4028/www.scientific.net/msf.575-578.1234.
- [21] D.K. Fidaros et al. “Numerical modelling of flow and transport processes in a calciner for cement production”. In: *Powder Technology* 171.2 (Feb. 2007), pp. 81–95. DOI: 10.1016/j.powtec.2006.09.011.
- [22] Hrvoje Mikulčić et al. “Numerical evaluation of different pulverized coal and solid recovered fuel co-firing modes inside a large-scale cement calciner”. In: *Applied Energy* 184 (Dec. 2016), pp. 1292–1305. DOI: 10.1016/j.apenergy.2016.05.012.
- [23] Hrvoje Mikulčić et al. “Numerical analysis of cement calciner fuel efficiency and pollutant emissions”. In: *Clean Technologies and Environmental Policy* 15.3 (Mar. 2013), pp. 489–499. DOI: 10.1007/s10098-013-0607-5.

- [24] Hrvoje Mikulčić et al. “The application of CFD modelling to support the reduction of CO₂ emissions in cement industry”. In: *Energy* 45.1 (Sept. 2012), pp. 464–473. DOI: 10.1016/j.energy.2012.04.030.
- [25] Hrvoje Mikulčić et al. “Numerical modelling of calcination reaction mechanism for cement production”. In: *Chemical Engineering Science* 69.1 (Feb. 2012), pp. 607–615. DOI: 10.1016/j.ces.2011.11.024.
- [26] KS Philips and Philips Enviro-Seal. *Case Study—M/S Maihar cement*. 2001.
- [27] N.A. Madloul et al. “An overview of energy savings measures for cement industries”. In: *Renewable and Sustainable Energy Reviews* 19 (Mar. 2013), pp. 18–29. DOI: 10.1016/j.rser.2012.10.046.
- [28] Ernst Worrell. “Energy efficiency improvement opportunities for the cement industry”. In: (2008).
- [29] Ali Hasanbeigi, Christoph Menke, and Apichit Therdyothin. “The use of conservation supply curves in energy policy and economic analysis: The case study of Thai cement industry”. In: *Energy Policy* 38.1 (Jan. 2010), pp. 392–405. DOI: 10.1016/j.enpol.2009.09.030.
- [30] Thomas J. Santner, Brian J. Williams, and William I. Notz. “The Design and Analysis of Computer Experiments”. In: (2018). DOI: 10.1007/978-1-4939-8847-1.
- [31] Yun Zhang et al. “Aspen Plus-based simulation of a cement calciner and optimization analysis of air pollutants emission”. In: *Clean Technologies and Environmental Policy* 13.3 (Oct. 2010), pp. 459–468. DOI: 10.1007/s10098-010-0328-y.
- [32] Azad Rahman et al. “Aspen Plus Based Simulation for Energy Recovery from Waste to Utilize in Cement Plant Preheater Tower”. In: *Energy Procedia* 61 (2014), pp. 922–927. DOI: 10.1016/j.egypro.2014.11.996.
- [33] Cementos Argos. “Industrial plant data”. In: (2019).
- [34] Grzegorz Borsuk et al. “Numerical simulation of thermal-hydraulic processes in the riser chamber of installation for clinker production”. In: *Archives of Thermodynamics* 37.1 (Mar. 2016), pp. 127–142. DOI: 10.1515/aoter-2016-0009.
- [35] Zhao Liu et al. “Optimal control for thermal energy efficiency of the cement clinker”. In: *Proceedings of the 37th Chinese Control Conference* (July 2018), pp. 25–27.
- [36] Pirooz Darabi. “A mathematical model for cement kilns”. MA thesis. Sharif University of Technology, Iran, Jan. 2004.
- [37] Kaustubh S. Mujumdar, Amit Arora, and Vivek V. Ranade. “Modeling of Rotary Cement Kilns: Applications to Reduction in Energy Consumption”. In: *Industrial & Engineering Chemistry Research* 45.7 (Mar. 2006), pp. 2315–2330. DOI: 10.1021/ie050617v.

- [38] Wei Shao et al. “Numerical simulation of heat transfer process in cement grate cooler based on dynamic mesh technique”. In: *Science China Technological Sciences* 59.7 (June 2016), pp. 1065–1070. DOI: 10.1007/s11431-016-6074-6.
- [39] Ursula Kääntee et al. “Modelling a cement manufacturing process to study possible impacts of alternative fuels”. In: *TMS Fall 2002 Extraction and Processing Division Meeting on Recycling and Waste Treatment in Mineral and Metal Processing: Technical and Economic Aspects*. June 2002.
- [40] Adem Atmaca and Recep Yumrutaş. “Analysis of the parameters affecting energy consumption of a rotary kiln in cement industry”. In: *Applied Thermal Engineering* 66.1-2 (May 2014), pp. 435–444. DOI: 10.1016/j.applthermaleng.2014.02.038.
- [41] Kurt E Peray and Joseph J Waddell. *The rotary cement kiln*. Edward Arnold, 1986.
- [42] Ernesto Barrios Zamudio. “Using the BsMD Package for Bayesian Screening and Model Discrimination”. In: (2013).
- [43] Richard E Rosenthal. “GAMS—a user’s guide”. In: (2004).
- [44] Arne Drud. “CONOPT: A GRG code for large sparse dynamic nonlinear optimization problems”. In: *Mathematical Programming* 31.2 (June 1985), pp. 153–191. DOI: <https://doi.org/10.1007/BF02591747>.